

Technical note: Quantifying size and shape of entheses

C.Y. HENDERSON^{1*}

¹CIAS—Research Centre for Anthropology and Health, University of Coimbra, Coimbra, Portugal

Received 14 June 2012; accepted 17 October 2012

Abstract Enteseal changes (ECs) have been widely recorded using visual methods, but size and shape affect stress distribution which cannot be quantified visually. The aim of this paper is to present a simple method for quantifying size and shape by applying parameters to quantify shape and to highlight preliminary results indicating that this method provides useful data. Hypotheses tested were: common extensor origin size correlates with humerus size; ECs change the size and shape of entheses; surface area is increased in those entheses with bony proliferation. The common extensor origins of 43 male skeletons from medieval York were recorded. The entheses were recorded visually for any deviation from a smooth surface. The chord was measured using sliding calipers and the shape of the entheses recorded using a profile gauge and quantified using parameters (e.g. the standard deviation of the surface from a mean line) which assess the relationship of the surface to a flat surface. To test replicability, disarticulated humeri were also recorded (inter-observer error $n = 9$; intra-observer error $n = 20$) using the same methodology. Replicability for size and shape was good for intra-observer error but weaker for inter-observer error. There is variability in entheses size and distal humeral condyle size; normal entheses are smaller than those with EC while their surface shape differs and is affected by the type of EC (proliferative or destructive); surface area in those entheses with proliferative ECs is increased. The use of these parameters for quantifying entheses size and shape provides insights into entheses variability which cannot be tested using visual methods alone. These parameters can be re-recorded using this two-dimensional method or can be measured on data collected with a laser scanner. Future research will test the relationship between surface size/shape and the effects of biological sex, age and occupation.

Key words: Common extensor origin, enteseal change (EC), musculoskeletal stress marker (MSM), enthesesopathy

Introduction

Enteseal changes (ECs), formerly called musculoskeletal stress markers (MSMs) (Jurmain and Villotte, 2010), are changes (sometimes pathological) to the attachment sites of tendons and ligaments to the skeleton. They have been widely used to infer activity patterns and they are normally scored visually, either as the presence of changes (Al-Oumaoui et al., 2004; Cardoso, 2008; Alves Cardoso and Henderson, 2010; Villotte et al., 2010) or on a scale of expression (Hawkey and Merbs, 1995; Chapman, 1997; Peterson, 1998; Steen and Lane, 1998; Weiss, 2003, 2007; Eshed et al., 2004; Jordana et al., 2006; Mariotti, et al., 2004, 2007; Molnar, 2006, 2010; Lieverse et al., 2008; Wysocki and Whittle, 2000; Henderson et al., 2012). Two- and three-dimensional studies of ECs have also been undertaken

(Wilczak, 1998; Zumwalt, 2005; Pany et al., 2009; Nolte and Wilczak, 2012). The only previous two-dimensional study quantified surface area from the chords of the surface but did not take into account surface curvature (Wilczak, 1998). The other studies have all quantified surfaces in three dimensions: one study used finite-element analysis to quantify surface complexity (Zumwalt, 2005), another the surface area (Nolte and Wilczak, 2012), and one calculated a variety of parameters including the deviation of the surface from a mean surface (Rq) for pectoralis major (a fibrous insertion). However, the relationship between entheses size, shape, and the direction of most variability in these parameters have not been fully explored, and further work on quantitative methods has been recommended to better understand ECs (Jurmain et al., 2012).

Visual methods for recording ECs, although widely used, do not provide detail on either the size or shape of entheses (but some methods do quantify, on an ordinal scale, the size of proliferative changes: e.g. Hawkey and Merbs, 1995). The geometry of entheses affects stress distribution and may, therefore, predispose some individuals to trauma at these sites, which may lead to ECs. This can only be studied by quantifying the size and shape of normal entheses and comparing them to those with ECs. ECs also change the

* Correspondence to: C.Y. Henderson, CIAS—Centro de Investigação em Antropologia e Saúde, Departamento de Ciências da Vida, FCTUC Universidade de Coimbra, Apartado 3046, 3001-401 Coimbra, Portugal.

E-mail: c.y.henderson@uc.pt

Published online 27 December 2012

in J-STAGE (www.jstage.jst.go.jp) DOI: 10.1537/ase.121017

shape of entheses, often by the production of bone spurs at the margins. These are likely to increase the surface area for attachment, thereby distributing loads over a greater area and thus reducing point loads. Therefore, quantification of shape allows new hypotheses to be tested, e.g. whether new bone formation increases surface area, and whether entheses size and shape is proportional to the size of the individual. Answering these questions may provide further insights into the aetiology of these changes, thereby improving our understanding of entheses and the use of ECs as indicators of activity-related stress.

The aim of this technical note is to present a novel and reproducible method for quantifying the surface shape of the common extensor origin (CEO) and to present preliminary data demonstrating the value of quantifying its size and shape. The following hypotheses are tested: (1) CEO size is proportional to humerus size (condylar width is used as a proxy for this), which would be expected as muscles, bones, and joints form a functional unit and discrepancies in size may lead to injury; (2) ECs change the size and shape of entheses, as would be expected if areas of attachment are removed or added; (3) new bone formation increases the surface area of the enthesis, particularly that occurring at the lateral margin which may form as an adaptation, thereby increasing area or changing the moment arm of the tendon.

Materials and Methods

Disarticulated humeri curated in the Fenwick Human Osteology Laboratory, Durham University, were used to determine both the inter- and intra-observer error. Intra-observer error was tested by recording 20 humeri, using the method defined below, two weeks after they were initially recorded without sight of the original recording forms. Inter-observer error was tested by a colleague who chose nine of these humeri. This colleague had no previous experience of recording entheses, but had more than five years experience of recording human skeletal remains.

All adult male skeletons from the late medieval (14th–15th century AD) site of Fishergate House, York, UK (Holst, 2005) were recorded ($n = 43$). The original report was used to select adult male skeletons (Holst, 2005). Only male individuals were used to avoid possible sex differences in enthesis size and shape, which will be tested in the future.

The CEO, a fibrocartilaginous enthesis, was chosen because it is regularly used for studies of activity-related stress and the soft tissues attaching at this site have been well studied (Greenbaum et al., 1999; Putz et al., 2003; Milz et al., 2004; Tsuji et al., 2008). Anatomical differences between fibrous and fibrocartilaginous entheses have only recently been acknowledged by those studying activity-related stress (Henderson, 2008; Alves Cardoso and Henderson, 2010; Villotte et al., 2010) but should be recognized when developing recording methods (Jurmain et al., 2012). Fibrocartilaginous entheses are composed of four layers of tissue from the soft to the hard, each with differing biomechanical properties (Benjamin and Ralphs, 1998; Thomopoulos et al., 2003). The first zone is that of the soft tissue (tendon, ligament, or joint capsule) followed by the zone of unmineralized fibrocartilage (Benjamin and Ralphs, 1998). In this

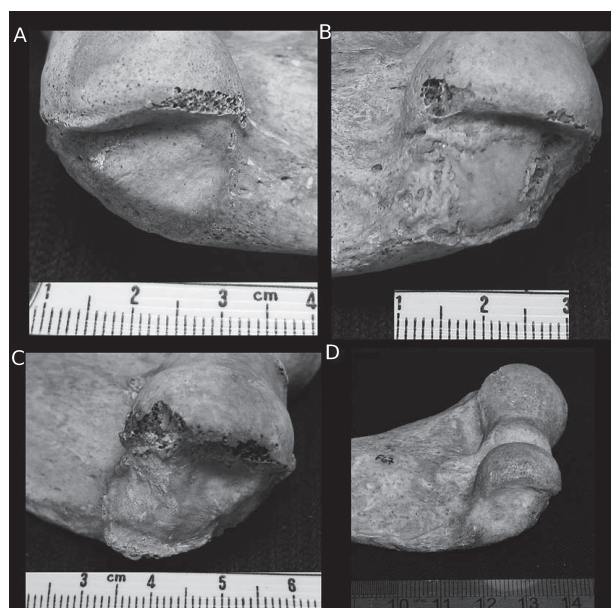


Figure 1. Common extensor origins demonstrating (A) normal common extensor origin, F209 left side; (B) other changes, this example has lytic and proliferative changes, F86 right side; (C) bone proliferation, F164 right side; (D) lytic change, F67 right side.

zone the collagen fibre orientation is altered so that they lie almost perpendicular to the enthesis which probably reduces bending stresses at the enthesis (Benjamin and Ralphs, 1998). The tidemark divides the zone of unmineralized tissue from the mineralized fibrocartilage below and, as with synovial joints, this is the zone retained after skeletons are macerated (François et al., 2001). Below the zone of mineralized fibrocartilage is the bone which interdigitates with the zone above, thereby increasing surface area, improving stress dissipation and reducing shearing forces between the zones (Benjamin and Ralphs, 1998).

The key feature of fibrocartilaginous entheses for visual recording is that the tidemark, like the tidemark in synovial joints, leaves a smooth footprint very distinct from the surrounding bone. This enables the margins of the enthesis to be clearly visualized and means that any deviation from this normal smooth surface, e.g. the presence of new bone formation, macroporosity, or lytic lesions, is recorded as an EC. This definition is common to this and other recent methods (Henderson et al., 2010, 2012; Villotte et al., 2010). For this study two sets of categories were defined. The first set was normal or abnormal and for the second set the abnormal entheses were split into three sub-categories: new bone formation, lytic lesions, and 'other,' which included mixed lesions (Figure 1). Skeletons with potential bone-forming diseases, e.g. diffuse idiopathic skeletal hyperostosis or the seronegative spondyloarthropathies (Henderson, 2008), were included in this study because these diseases are not considered developmental (Ortner, 2003); therefore, they should not influence the size or shape of the enthesis.

Measurements were taken of the maximum width of the humeral condyle as defined in Buikstra and Ubelaker (1994). Two perpendicularly bisecting chords of the enthesis

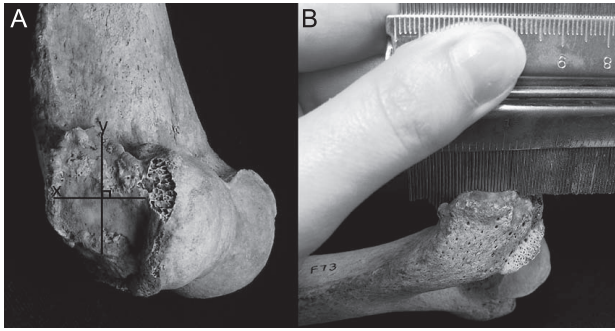


Figure 2. Common extensor origin demonstrating x and y axes of F73 right side: (A) chord x and y , $x = 15.46$ mm, $y = 20.49$ mm; (B) profile gauge held against y axis. Scale on profile gauge.

were measured using digital sliding calipers. The chords were measured mediolaterally (x axis) and proximodistally (y axis) (Figure 2). This has previously been undertaken to study the size of attachments to improve surgical reattachment (Minagawa et al., 1998; Curtis et al., 2006; Mazzocca et al., 2007; Forthman et al., 2008). In addition, the surface roughness was recorded along the same x and y axes using a profile gauge with 0.8 mm prong width (Figure 2B) (Henderson and Gallant, 2007; Henderson, 2009). The profile gauge was transferred from the bone to enable a line to be drawn on paper within a grid (to avoid changing orientation). These lines were then scanned on a flatbed scanner at a line resolution of 10 pixels per cm and rotated to ensure that the left and right sides could be compared (Henderson and Gallant, 2007; Henderson, 2009). Surface roughness parameters were then used to quantify the shape of these lines using a routine written in Octave (version 3.0.2). It is important to note that although these parameters are widely used in materials science to quantify surface roughness (Scarr, 1967; Lin and Hopfe, 1986; Gadelmawla et al., 2002) they are, due to the resolution of the profile gauge, being used to quantify the overall shape of the enthesis, i.e. how it differs from a flat surface. This paper will focus on three of these parameters calculated: root mean square roughness (Rq), peak number (g) and relative length (l_o) (defined in Table 1). Amplitude of the curve is measured using Rq which is the standard deviation of the surface from the mean line. Lower values of Rq indicate that the standard deviation is closer to the mean line, i.e. the surface is flatter. Horizontal variation was measured using peak number, which calculates the number of inflection points (the point at which the curve changes direction). Lower values for this parameter indicate fewer peaks. Finally, relative length is a hybrid parameter measuring both horizontal and vertical variation, and is the total length of the curve divided by the chord (which is measured in pixels within the Octave routine): a flat enthesis will have a value of 1, while a parabolic enthesis will have a value > 1 .

All statistical tests were calculated using SPSS version 14. Intra-observer error was tested using Spearman's rho, while, because of the limited sample size ($n = 9$), inter-observer error was tested using Kendall's tau. The technical

Table 1. The surface roughness parameters along with their definitions, using the standard denotations (Rq , g , and l) for these parameters.

Parameter	Definition
Root mean square roughness (Rq)	Standard deviation of the distribution of surface heights. $Rq = \sqrt{\frac{1}{n} \sum_{i=1}^n y_i^2}$
Peak number (PeakNum)	Number of points where the curve changes direction (d) per unit length (L) $g = \frac{1}{L} \sum_{i=1}^n d_i$
Relative length (Rellength)	Calculated by a summation of the lengths (l) of the individual parts of the profile divided by the assessment length (L) $l_o = \frac{1}{L} \sum_{i=1}^n l_i$

error measurement ($TEM = \sqrt{\frac{\sum D^2}{2N}}$) and coefficient of reliability

$\left(1 - \left(\frac{TEM^2}{SD^2}\right)\right)$ were also calculated for both intra- and

inter-observer error to evaluate the overall variation between the observations. Descriptive statistics were used to demonstrate normal and abnormal variation. Pearson tests and Spearman tests (for the small sample sizes) were used to determine whether the chord of the enthesis (x or y axis) or relative length demonstrated a linear relationship with condylar width. Further statistical tests were not undertaken due to the small sample size. To increase the initial sample size, left and right sides were used, but not both from the same individual. Where both were recordable in the same individual the side chosen for this study was randomly selected. This does not affect the results, as no hypotheses regarding individual variation or differences between left and right sides were being tested.

Results

Intra-observer error (Table 2) was low, with a high correlation (e.g. peak number has a Spearman's rho = 0.540, $P = 0.014$) between first and second measurement (Table 2). Inter-observer (Table 3) error was poorly correlated for the measurements of the chords (x axis, Spearman's rho = 0.13, $P = 0.54$; y axis Spearman's rho = 0.21, $P = 0.33$) and Rq (Spearman's rho = 0.222, $P = 0.404$) but demonstrated significant correlations for peak number (Spearman's rho = 0.667, $P = 0.012$) and relative length (Spearman's rho = 0.611, $P = 0.022$). The differences in correlation for these parameters may be caused by the greater variability of scores than for peak number or relative length (Table 3) or the sensitivity of this parameter to changes in slope which may occur if the horizontal axis of the profile gauge is misaligned with the gridded paper. The TEM and rho for both

Table 2. Intra-observer error: descriptive statistics and correlation

	<i>n</i>	Minimum	Maximum	Mean	SD	Skewness	Skewness SE	Kurtosis	Kurtosis SE	Spearman's rho		rho
										Correlation coefficient	significance	
chord <i>x</i>	20	9.28	31.32	12.84	4.09	4.09	0.46	18.96	0.90	0.74	0.00	1.95
	20	7.61	14.75	12.28	1.72	-1.01	0.47	1.14	0.92			0.04
chord <i>y</i>	20	9.58	17.11	12.91	1.93	0.14	0.46	-0.39	0.89	0.82	0.00	0.66
	20	7.94	16.45	12.57	1.95	-0.27	0.46	0.21	0.89			0.67
<i>Rq</i>	20	1.939	11.112	5.355	2.629	0.709	0.512	-0.224	0.992	0.932	0.000	0.368
	20	1.601	11.866	5.303	2.625	0.756	0.512	0.623	0.992			0.82
Peak num	20	0.037	0.076	0.055	0.011	0.253	0.512	-0.681	0.992	0.540	0.014	7.09E-03
	20	0.035	0.096	0.055	0.016	1.206	0.512	1.430	0.992			0.997
Rel length	20	1.004	1.125	1.040	0.030	1.295	0.512	2.154	0.992	0.795	0.000	7.76E-03
	20	0.998	1.110	1.043	0.029	0.689	0.512	-0.023	0.992			0.996

Chord *x* and chord *y* are the measurements of the enthesis in mm (using sliding calipers accurate to 0.01 mm), the roughness parameters all refer to the *y* axis of the common extensor origin. TEM = technical error measurement, rho = coefficient of reliability.

Table 3. Inter-observer error: descriptive statistics and correlation

	<i>n</i>	Minimum	Maximum	Mean	SD	Skewness	Kurtosis	Kendall's tau		rho		
								Correlation coefficient	significance			
chord <i>x</i>	Observer 1	13	10.64	14.50	12.22	0.94	0.52	0.13	0.54	1.06	0.44	
	Observer 2	13	8.57	15.47	12.85	2.13	0.05					
chord <i>y</i>	Observer 1	13	9.58	14.84	12.51	1.62	-1.22	0.21	0.33	2.87	-1.59	
	Observer 2	13	10.98	20.70	17.46	2.75	0.71					
<i>Rq</i>	Observer 1	9	4.385	15.291	8.631	4.320	-1.417	0.222	0.404	2.07	-0.108	
	Observer 2	9	4.635	17.374	10.602	3.898	-0.154	0.667	0.012	4.21E-03	0.998	
PeakNum	Observer 1	9	0.029	0.056	0.039	0.010	0.753	-0.686				
	Observer 2	9	0.022	0.057	0.038	0.013	0.330	-1.670				
Rellen	Observer 1	9	1.051	1.340	1.178	0.093	0.505	-0.497	0.611	0.022	3.58E-02	0.983
	Observer 2	9	1.070	1.256	1.161	0.067	-0.117	-1.462				

Chord *x* and chord *y* are the measurements of the enthesis in mm (using sliding calipers accurate to 0.01 mm), the roughness parameters all refer to the *y* axis of the common extensor origin. Observer 1 refers to the author. TEM = technical error measurement and rho = coefficient of reliability.

Table 4. Descriptive statistics: Common extensor origin (CEO) *x* axis

Category	Measure	<i>n</i>	Minimum	Maximum	Mean	SD
Normal (1)	<i>Rq</i>	11	0.379	0.952	0.667	0.187
	RelLength	11	0.998	1.027	1.009	0.009
	PeakNum	11	0.054	0.084	0.069	0.008
	condylar width	12	39.96	50.68	46.27	2.80
	CEO: <i>x</i>	11	10.31	15.83	13.21	1.89
EC other (21)	<i>Rq</i>	4	0.699	1.884	1.296	0.485
	RelLength	4	1.005	1.036	1.019	0.013
	PeakNum	4	0.062	0.068	0.064	0.003
	condylar width	4	44.96	49.67	47.67	1.97
	CEO: <i>x</i>	4	12.71	16.70	13.91	1.87
Proliferative (22)	<i>Rq</i>	15	0.533	1.194	0.892	0.205
	RelLength	15	1.004	1.034	1.020	0.009
	PeakNum	15	0.059	0.080	0.067	0.006
	condylar width	15	41.16	54.24	47.45	3.77
	CEO: <i>x</i>	15	6.57	16.24	13.03	2.41
Lytic (23)	<i>Rq</i>	1	1.061	1.061	n/a	n/a
	RelLength	1	1.009	1.009	n/a	n/a
	PeakNum	1	0.076	0.076	n/a	n/a
	condylar width	1	52.16	52.16	n/a	n/a
	CEO: <i>x</i>	1	13.83	13.83	n/a	n/a
All EC categories pooled (4)	<i>Rq</i>	20	0.533	1.884	0.981	0.309
	Rel length	20	1.004	1.036	1.019	0.009
	Peak num	20	0.059	0.080	0.067	0.006
	condylar width	20	41.16	54.24	47.73	3.49
	CEO: <i>x</i>	20	6.57	16.70	13.25	2.23

peak number and relative length, for both intra- and inter-observer error, indicate good reliability, perhaps due to the limited variability in these scores. The reliability is less good for the other measures. These results indicate that not only is the alignment an issue, but also the identification of the margins of both the profile gauge and the sliding calipers.

For the preliminary study, using the skeletons from Fishergate (Appendix 1), the sample size for the *x* axis was smaller than for the *y* axis (Table 4, Table 5). This is because measurement or profiles of the *x* axis could not be made accurately when there was post-mortem damage to the most lateral aspect of the enthesis—the most common location for damage to the CEO. The effect of post-mortem damage is a limitation of this method, but is also a limitation for all methods used to record ECs.

Only normal entheses were used to test the first hypothesis, i.e. that enthesis size correlated with humerus size. No correlations were found between the condylar width and the measurements of the chords, or for the relative length of the *x* or *y* axes (Table 6). This is demonstrated by the scatter plots (Figure 3) which indicate that there is normal variation in enthesis size compared to condylar width.

All entheses were used to test the second hypothesis, i.e. ECs affect the size and shape of entheses. The chords of normal entheses (category 1) were on average marginally smaller than entheses with ECs (all ECs pooled, category 4) in both *x* and *y* dimensions (Table 4, Table 5), but it is worth noting that entheses with changes have a wider range of sizes. This may reflect the larger number of cases with ECs.

For measures of shape, using the parameters *Rq* and relative length, both *x* and *y* axes of normal entheses (category 1)

have mean values smaller than those with ECs (category 4) (Table 4, Table 5). The peak number, for both axes, demonstrates the opposite trend. Due to the small sample size of normal entheses it is not possible to draw substantive conclusions regarding these findings.

The differences described above are for all types of ECs. Table 4 and Table 5 demonstrate that there are differences in size and shape when the categories of ECs are differentiated. For those with proliferative changes (category 22), which represent the majority of cases (*n* = 15), the mean values of chord *y* and the condylar width are larger than the normal entheses. The mean values of the shape parameters are generally larger for those with proliferative changes than the normal entheses, except for the peak number in both *x* and *y* axes which is smaller for those with these changes. For the lytic changes (*n* = 1), no conclusions can be drawn, but both chords and condylar width are larger in those with lytic changes. In the *x* axis both *Rq* and peak number are larger in those with lytic changes, while relative length is identical. In the *y* axis, relative length is larger in those with lytic changes, while the *Rq* and peak number are larger in those without changes. Finally, those entheses with mixed ECs (*n* = 4), have larger mean values for the chords, condylar width and *Rq* in both *x* and *y* axes, as well as for the relative length of the *x* axis. The mean values of the peak number for the *x* and *y* axes are smaller, and in the *y* axis the relative length is identical. These data support the second hypotheses, i.e. that ECs change the size and shape of entheses.

All entheses were used to test the third hypothesis, i.e. that surface area was increased in those entheses with proliferative changes compared to normal entheses and those with

Table 5. Descriptive statistics: Common extensor origin (CEO) *y* axis

Category	Measure	<i>n</i>	Minimum	Maximum	Mean	SD
Normal (1)	<i>Rq</i>	12	0.336	1.293	0.548	0.255
	Rel length	12	1.002	1.032	1.013	0.009
	Peak num	12	0.058	0.081	0.068	0.007
	condylar width	12	39.96	50.68	46.27	2.80
	CEO: <i>y</i>	12	11.30	16.67	14.78	1.48
EC other (21)	<i>Rq</i>	4	0.410	0.963	0.633	0.234
	Rel length	4	1.008	1.018	1.013	0.004
	Peak num	4	0.052	0.073	0.064	0.010
	condylar width	4	44.96	49.67	47.67	1.97
	CEO: <i>y</i>	4	14.92	18.11	16.65	1.60
Proliferative (22)	<i>Rq</i>	15	0.309	0.969	0.592	0.203
	Rel length	15	1.005	1.028	1.017	0.007
	Peak num	15	0.060	0.072	0.066	0.004
	condylar width	15	41.16	54.24	47.45	3.77
	CEO: <i>y</i>	15	10.04	19.42	15.47	2.94
Lytic (23)	<i>Rq</i>	1	0.474	0.474	n/a	n/a
	Rel length	1	1.015	1.015	n/a	n/a
	Peak num	1	0.058	0.058	n/a	n/a
	condylar width	1	52.16	52.16	n/a	n/a
	CEO: <i>y</i>	1	17.09	17.09	n/a	n/a
All EC categories pooled (4)	<i>Rq</i>	20	0.309	0.969	0.595	0.200
	Rel length	20	1.005	1.028	1.016	0.007
	Peak num	20	0.052	0.073	0.065	0.005
	condylar width	20	41.16	54.24	47.73	3.49
	CEO: <i>y</i>	20	10.04	19.42	15.79	2.67

Table 6. Correlations between enthesis size and shape and condylar width, where category 1 are normal entheses and 4 are those with Ecs

Category	Measurement	Statistic	CEO: <i>x</i> (mm)	Relative length (<i>x</i>)	Category	Measurement	Statistic	CEO: <i>y</i> (mm)	Relative length (<i>y</i>)
1	Condylar width (mm)	Spearman	-0.128	0.358	1	Condylar width (mm)	Spearman	0.545	0.266
		Sig. (two-tailed)	0.725	0.31			Sig. (two-tailed)	0.067	0.404
		<i>n</i>	10	10			<i>n</i>	12	12
CEO: <i>x</i> (mm)	Spearman	Spearman	1	-0.032	CEO: <i>y</i> (mm)	Spearman	Spearman	1	0.084
		Sig. (two-tailed)		0.926			Sig. (two-tailed)		0.795
		<i>n</i>	11	11			<i>n</i>	12	12
4	Condylar width (mm)	Pearson	0.465*	-0.015	4	Condylar width (mm)	Pearson	0.656**	0.297
		Sig. (two-tailed)	0.045	0.951			Sig. (two-tailed)	0.002	0.204
		<i>n</i>	19	19			<i>n</i>	20	20
CEO: <i>x</i> (mm)	Pearson	Pearson	1	0.219	CEO: <i>y</i> (mm)	Pearson	Pearson	1	0.205
		Sig. (two-tailed)		0.354			Sig. (two-tailed)		0.387
		<i>n</i>	19	20			<i>n</i>	20	20

* Correlation is significant at the 0.05 level (two-tailed).

** Correlation is significant at the 0.01 level (two-tailed).

other types of changes. This was tested using the parameter relative length. As can be seen from Figure 4 and Figure 5, Table 4 and Table 5, relative length is larger in both *x* and *y* axes compared to normal and compared to those with lytic (category 23) and other (category 21) types of changes. Therefore, this hypothesis is supported.

Discussion

The aim of this paper was to demonstrate that enthesis size and shape could be meaningfully quantified to test hypotheses concerning size and shape variation. While visual

methods have dominated the field (for a review, see Jurmain et al., 2012) the size and shape, particularly the normal variation, have not been studied, and these both affect stress distribution. Consequently, it is important to understand normal variation to improve interpretation of ECs by understanding their effect on stress distribution. Understanding what affects enthesis size and shape will also improve interpretation of ECs recorded using visual methods. This new method measures the chord of the enthesis using sliding calipers and is, therefore, a method that can be widely applied. The method for recording surface shape presented here requires very little equipment, but is low resolution and slow to process.

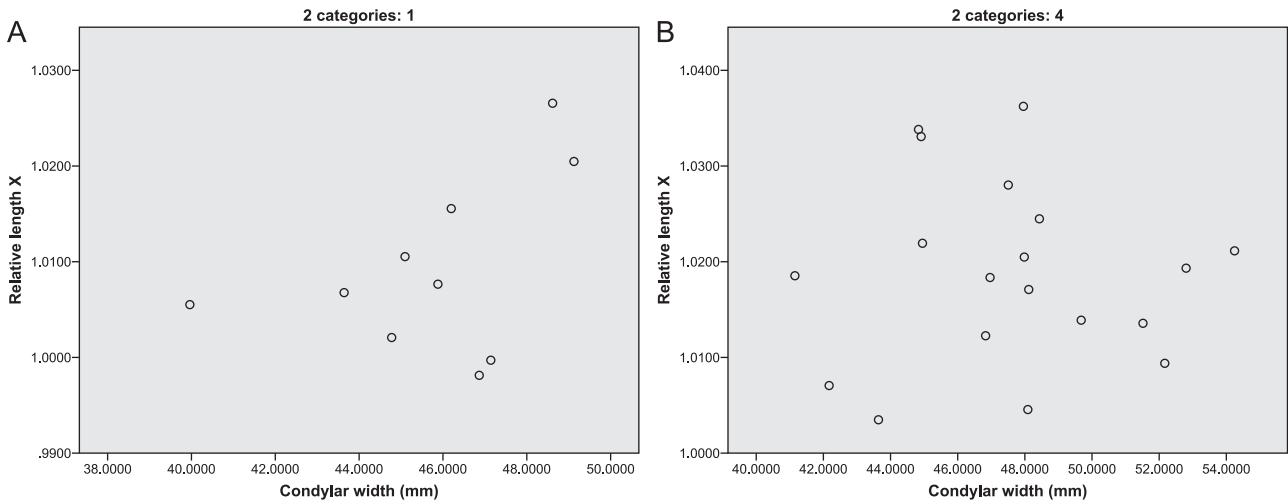


Figure 3. Scatterplots of common extensor origin size and condylar width: (A) normal relative length; (B) all enthesal changes, relative length.

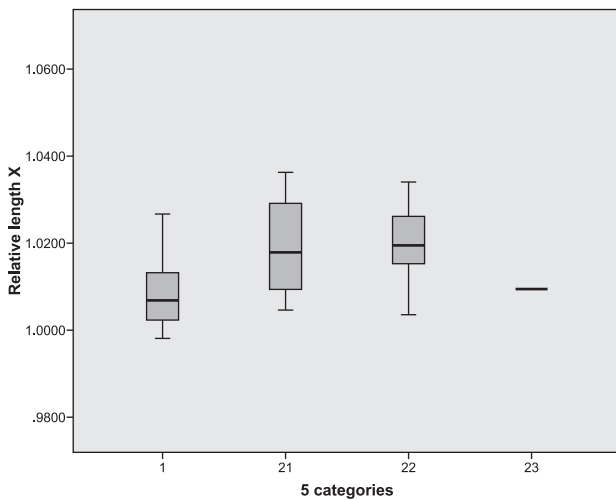


Figure 4. Common extensor origin *x* relative length variation with enthesal change status (1 = normal, 21 = EC other, 22 = EC proliferative, 23 = EC destructive). Data presented excludes the right common extensor origin of F28 which was an outlier. Histogram indicates range and median.

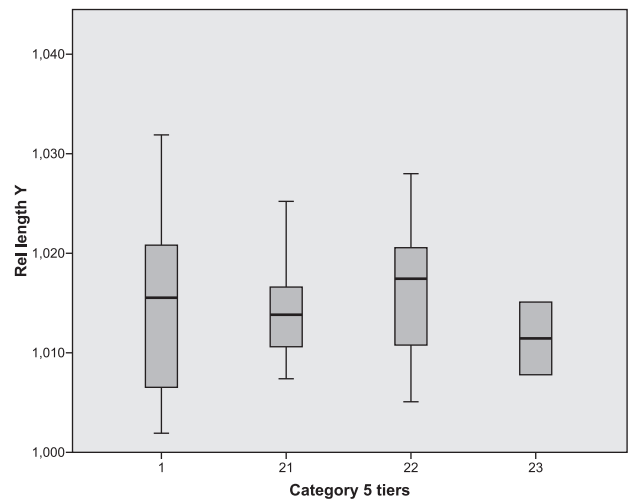


Figure 5. Common extensor origin *y* relative length variation with enthesal change status (1 = normal, 21 = EC other, 22 = EC proliferative, 23 = EC destructive). Histogram indicates range, median and outliers.

However, the method for quantifying the shape is widely applicable and can be used on data collected using three-dimensional laser scanners on three-dimensional data. Three-dimensional data can also be collected and then transformed to study two axes bisecting perpendicularly to resolve questions as to where most shape variation occurs to study the plasticity of entheses. It should also be noted that, once the data is collected, whether using a profile gauge or a three-dimensional laser scanner, other parameters (Gadelmawla et al., 2002) can be applied to study surface shape variation or at high resolution can be utilized to quantify surface roughness.

Intra-observer error for the measurement of the chords of the enthesis and for the surface roughness parameters was

low, with high correlations between the first and second observations. Inter-observer error, in contrast, was higher. This has also been found to be a problem for visual recording methods (Henderson et al., 2010, 2012; Davis et al., 2012b). The new 'Coimbra method' for recording entheses reported a low of 65.3% agreement and a high of 78.1% agreement between scorers, all of whom had considerable experience of recording ECs and were involved in developing the method (Henderson et al., 2010). Intra-observer error for that method ranged between 66.8% (Achilles tendon insertion) and 82.7% (CEO), depending on enthesis. Davis et al. (2012a) tested two methods using only publications as guides. Those recording had varying levels of experience of recording ECs. They found low levels of agreement which were not

dependent on the level of experience of the observer, but were dependent on the levels of variability of ECs at entheses. Therefore, the very weak correlations are not substantially worse than for visual recording methods and, given the good correlations for intra-observer error, would probably improve with lengthier training.

The limited sample size, due to the preliminary nature of this study, means that the findings should be considered with caution, but that interesting trends may be present which require confirmation with a higher-resolution study of a larger sample. The chords of entheses demonstrated that entheses size does not correlate with condylar width, which was used as a proxy for humerus size. This may reflect differential effects of development on joint growth compared to entheses growth and warrants further study. Chord length was typically larger, in both x and y axes, for entheses with abnormalities. This was an unexpected finding, because larger entheses have a larger surface area and should therefore be less prone to stress-induced changes. However, the chord does not describe the actual size of the surface; therefore, relative length was used to interpret these findings. Relative length measures how the real length (pixels) of the entheses (for this two-dimensional study how long the line drawn would be if it were stretched out) relates to the chord length (in pixels). A value > 1 for relative length indicates that the entheses length is longer than the chord, thus this measurement can be used to indicate increased surface area along an axis. Relative length, like chord length, was found to have an increased mean value for those entheses with ECs. However, unlike chord length, this was not the case for the x axis for those with lytic changes or for the y axis for those with mixed changes. However, the very limited sample size ($n = 1$) for those entheses with lytic lesions means that a larger sample size is required to confirm this finding. This demonstrates that, while chord length is useful, it does not provide the full picture. However, relative length did not correlate with condylar width for either axis for normal entheses. This supports the idea that joint size, as measured by condylar width, and entheses size are affected by different developmental processes, perhaps unsurprising given that the CEO is the entheses for muscles controlling the hand and wrist and not the elbow. Future research should compare the size of the entheses with size of the joints upon which the muscles act.

The root mean square roughness (Rq) measures the amplitude of entheses shape by calculating its standard deviation from its mean line, i.e. lower values of Rq indicate flatter surfaces. The mean values for the x and y axes demonstrated flatter surfaces for normal entheses compared to those with ECs. The y axis is always flatter than the x axis, which may indicate that surface shape is more plastic mediolaterally (x axis) compared to proximodistally (y axis). Peak number calculates the number of inflection points: a higher number indicates a surface with more inflection points. Peak number was typically higher for the normal entheses (note that the range was more variable) than those with most types of changes and was typically higher in the x than the y axis. Hence normal surfaces have more inflection points as does the x axis compared to the y axis. Further studies are required on a larger sample to interpret these findings.

The hypotheses tested using these methods demonstrated that the CEO is not proportional to condylar width, that ECs do change both the size and shape of entheses, and that new bone formation increases the surface area of the entheses. The latter finding indicates that new bone formation increases surface area, thereby decreasing point loading and may, therefore, be a useful adaptation. This small study demonstrates the value of quantifying surface size and shape and should be tested further using higher-resolution technology on identified individuals, i.e. those of known sex, age, and occupation, to study sexual differences and the effects of age and activity patterns on entheses size and shape. Once the 'Coimbra method' (Henderson et al., 2012) has been fully developed and tested further, the relationship between types of ECs (as defined by that method) and size and shape should be studied.

Conclusions

This preliminary study has demonstrated the value of recording size and shape, whether this is by measuring the chord of the entheses using sliding calipers or using a profile gauge and parameters which quantify shape. Intra-observer error was low, but inter-observer error was higher, indicating that prior to widespread application of this technique, training is required to identify the midpoints of entheses and their margins. The hypothesis that CEO was proportional to condylar width was not supported. However, ECs were found to change the size and shape of entheses and bone proliferation was found to increase the surface area. Future research should test these hypotheses on larger sample sizes, ideally using a three-dimensional laser scanner to improve the resolution of the data.

Acknowledgments

The data in this paper were collected while the author was a Ph.D. student at the Department of Archaeology, Durham University. The author wishes to thank Dr. A.J. Gallant of the School of Engineering and Computing Sciences, Durham University for advice on programming. I would also like to thank the three anonymous reviewers for their useful comments.

Grant sponsorship: FCT—Fundação para a Ciência e a Tecnologia, reference: SFRH/BPD82559/2011.

References

- Al-Oumaoui I., Jiménez-Brobeil S., and du Souich P. (2004) Markers of Activity Patterns in some Populations of the Iberian Peninsula. *International Journal of Osteoarchaeology*, 14: 343–359.
- Alves Cardoso F. and Henderson C.Y. (2010) Enthesopathy formation in the humerus: data from known age-at-death and known occupation skeletal collections. *American Journal of Physical Anthropology*, 141: 550–560.
- Benjamin M. and Ralphs J.R. (1998) Fibrocartilage in tendons and ligaments—an adaptation to compressive load. *Journal of Anatomy*, 193: 481–494.
- Buikstra J.E. and Ubelaker D.H. (1994) Standards for Data Collection from Human Remains. *Arkansas Archeological Survey Research Series*, No. 44, Fayetteville.

- Cardoso F.A. (2008) A Portrait of Gender in Two 19th and 20th Century Portuguese Populations: A Palaeopathological Perspective. Ph.D. thesis, Durham University.
- Chapman N.E.M. (1997) Evidence for Spanish influence on activity induced musculoskeletal stress markers at Pecos Pueblo. *International Journal of Osteoarchaeology*, 7: 497–506.
- Curtis A.S., Burbank K.M., Tierney J.J., Scheller A.D., and Curran A.R. (2006) The insertional footprint of the rotator cuff: an anatomic study. *Arthroscopy*, 22: 603–609.
- Davis C.B., Shuler K., Danforth M.E., and Herndon K. (2012a) Let's get real about MSMs: reliability in scoring techniques. *American Journal of Physical Anthropology*, 147(S54): 126.
- Davis C.B., Shuler K., Danforth M.E., and Herndon K. (2012b) Patterns of interobserver error in the scoring of enthesal changes. *International Journal of Osteoarchaeology*, doi:10.1002/oa.2277.
- Eshed V., Gopher A., Galili E., and Hershkovitz I. (2004) Musculoskeletal stress markers in Natufian hunter-gatherers and neolithic farmers in the Levant: the upper limb. *American Journal of Physical Anthropology*, 123: 303–315.
- Forthman C.L., Zimmerman R.M., Sullivan M.J., and Gabel G.T. (2008) Cross-sectional anatomy of the bicipital tuberosity and biceps brachii tendon insertion: relevance to anatomic tendon repair. *Journal of Shoulder and Elbow Surgery*, 17: 522–526.
- François R.J., Braun J., and Khan M.A. (2001) Entheses and enthesitis: a histopathologic review and relevance to spondyloarthritides. *Current Opinion in Rheumatology*, 13: 255–264.
- Gadelmawla E.S., Koura M.M., Maksoud T.M.A., Elewa I.M., and Soliman H.H. (2002) Roughness parameters. *Journal of Materials Processing Technology*, 123: 133–145.
- Greenbaum B., Itamura J., Vangsness C.T., Tibone J., and Atkinson R. (1999) Extensor carpi radialis brevis: An anatomical analysis of its origin. *Journal of Bone and Joint Surgery (BR)*, 81: 926–929.
- Harris E.F. and Smith R.N. (2009) Accounting for measurement error: a critical but overlooked process. *Archives of Oral Biology*, 54S: 107–117.
- Hawkey D.E. and Merbs C.F. (1995) Activity-induced musculoskeletal stress markers (MSM) and subsistence strategy changes among ancient Hudson Bay Eskimos. *International Journal of Osteoarchaeology*, 5: 324–338.
- Henderson C. (2008) When hard work is disease: The interpretation of enthesopathies. In: Brickley M. and Smith M. (eds.), *Proceedings of the Eighth Annual Conference of the British Association for Biological Anthropology and Osteoarchaeology*. British Archaeological Reports International Series 1743, Archaeopress, Oxford, pp. 17–25.
- Henderson C. (2009) A quantitative method for assessing MSM rugosity. Workshop in Musculoskeletal Stress Markers (MSM): Limitations and Achievements in Reconstruction of Past Activity patterns, Coimbra, Portugal, 2–3 July 2009. Available to download at: http://www.uc.pt/en/cia/msm/oral_henderson
- Henderson C. and Gallant A.J. (2007) Quantitative recording of entheses. *Paleopathology Newsletter*, 137: 7–12.
- Henderson C., Mariotti V., Pany-Kucera D., Perreard-Lopreno G., Villotte S., and Wilczak C. (2010) Scoring enthesal changes: proposal of a new standardised method for fibrocartilaginous entheses [poster]. 18th European Meeting of the Paleopathology Association, 23–26 August 2010, Vienna. <https://www.uc.pt/en/cia/msm/Vienna2010.pdf>
- Henderson C.Y., Mariotti V., Pany-Kucera D., Perreard-Lopreno G., Villotte S., and Wilczak C. (2012) Recording specific features of fibrocartilaginous entheses: preliminary results of the Coimbra standard method. *International Journal of Osteoarchaeology*, doi:10.1002/oa.2287.
- Holst M. (2005) Artefacts and environmental evidence: the human bone. In: Spall C.A. and Toop N.J. (eds.), *Blue Bridge and Fishergate House, York. Report on Excavations: July 2000 to July 2002*. Archaeological Planning Consultancy Ltd., York. <http://www.archaeologicalplanningconsultancy.co.uk/mono/001/>
- Jordana X., Galtés I., Busquets F., Isidro A., and Malgosa A. (2006) Clay-shoveler's fracture: an uncommon diagnosis in palaeopathology. *International Journal of Osteoarchaeology*, 16: 366–372.
- Jurmain R. and Villotte S. (2010) Terminology. Entheses in medical literature and physical anthropology: a brief review [online]. http://www.uc.pt/en/cia/msm/MSM_terminology3
- Jurmain R., Alves Cardoso F., Henderson C., and Villotte S. (2012) Bioarchaeology's Holy Grail: the reconstruction of activity. In: Grauer, A. (ed.), *A Companion to Paleopathology*. Wiley/Blackwell: Chichester. pp. 431–542.
- Lieverse A.R., Metcalf M.A., Bazaliiskii V.I., and Weber A.W. (2008) Pronounced bilateral asymmetry of the complete upper extremity: a case from the early Neolithic Baikal, Siberia. *International Journal of Osteoarchaeology*, 18: 219–239.
- Lin C.C. and Hopfe H.H. (1986) A surface roughness characterization system. *Wear*, 109: 79–85.
- Mariotti V., Facchini F., and Belcastro M.G. (2004) Enthesopathies—proposal of a standardized scoring method and applications. *Collegium Anthropologicum*, 28: 145–159.
- Mariotti V., Facchini F., and Belcastro M.G. (2007) The study of entheses: proposal of a standardised scoring method for twenty-three entheses of the postcranial skeleton. *Collegium Anthropologicum*, 31: 291–313.
- Mazzocca A.D., Cohen M., Berkson E., Nicholson G., Carofino B.C., Arclero R., and Romeo A.A. (2007) The anatomy of the bicipital tuberosity and distal biceps tendon. *Journal of Shoulder and Elbow Surgery*, 16: 122–127.
- Milz S., Tischer T., Buettner A., Schieker M., Maier M., Redman S., Emery P., McGonagle D., and Benjamin M. (2004) Molecular composition and pathology of entheses on the medial and lateral epicondyles of the humerus: a structural basis for epicondylitis. *Annals of the Rheumatic Diseases*, 63: 1015–1021.
- Minagawa H., Itoi E., Konno N., Kido R., Sano A., Urayama M., and Sato K. (1998) Humeral attachment of the supraspinatus and infraspinatus tendons: an anatomic study. *Arthroscopy*, 14: 302–306.
- Molnar P. (2006) Tracing prehistoric activities: musculoskeletal stress marker analysis of a stone-age population on the island of Gotland in the Baltic Sea. *American Journal of Physical Anthropology*, 129: 12–23.
- Molnar P. (2010) Patterns of physical activity and material culture on Gotland, Sweden, during the Middle Neolithic. *International Journal of Osteoarchaeology*, 20: 1–14.
- Nolte M.L. and Wilczak C. (2012) Effects of age-at-death, sex, body size and secular change on the biceps enthesis: a study of 3D surface areas. *American Journal of Physical Anthropology*, 147(S54): 225.
- Ortner D. (2003) *Identification of Pathological Conditions in Human Skeletal Remains*. Academic Press: San Diego.
- Pany D., Viola T., and Teschler-Nicola M. (2009) The scientific value of using a 3D surface scanner to quantify entheses. Oral communication presented at the Workshop in Musculoskeletal Stress Markers (MSM): Limitations and Achievements in the Reconstruction of Past Activity Patterns. University of Coimbra, 2–3 July 2009. Available from: http://www.uc.pt/en/cia/msm/MSM_podium
- Peterson J. (1998) The Natufian hunting conundrum: spears, atlatls, or bows? Musculoskeletal and armature evidence. *International Journal of Osteoarchaeology*, 8: 378–389.
- Putz R., Milz S., Maier M., and Boszczyk A. (2003) Funktionelle Morphologie des Ellenbogengelenks. *Orthopäde*, 32: 684–690.
- Scarr A.J.T. (1967) *Metrology and Precision Engineering*. McGraw-Hill, London.
- Steen S.L. and Lane R.W. (1998) Evaluation of habitual activities among two Eskimo populations based on musculoskeletal

- stress markers. *International Journal of Osteoarchaeology*, 8: 341–353.
- Thomopoulos S., Williams G.R., Gimbel J.A., Favata M., and Soslowky L.J. (2003) Variation of biomechanical, structural, and compositional properties along the tendon to bone insertion site. *Journal of Orthopaedic Research*, 21: 413–419.
- Tsuji H., Wada R., Oda R., Iba K., Aoki M., Murakami G., and Yamashita T. (2008) Arthroscopic, macroscopic, and microscopic anatomy of the synovial fold of the elbow joint in correlations with the common extensor origin. *Arthroscopy: The Journal of Arthroscopic and Related Surgery*, 24: 34–38.
- Villootte S., Castex D., Couallier V., Dutour O., Knüsel C.J., and Henry-Gambier D. (2010) Enthesopathies as occupational stress markers: evidence from the upper limb. *American Journal of Physical Anthropology*, 142: 224–234.
- Weiss E. (2003) Understanding muscle markers: aggregation and construct validity. *American Journal of Physical Anthropology*, 121: 230–240.
- Weiss E. (2007) Muscle markers revisited: activity pattern reconstruction with controls in a central California Amerind population. *American Journal of Physical Anthropology*, 133: 931–904.
- Wilczak C.A. (1998) Consideration of sexual dimorphism, age, and asymmetry in quantitative measurements of muscle insertion sites. *International Journal of Osteoarchaeology*, 8: 311–325.
- Wysocki M. and Whittle A. (2000) Diversity, lifestyles and rites: new biological and archaeological evidence from British Earlier Neolithic mortuary assemblages. *Antiquity*, 74: 591–601.
- Zumwalt A.C. (2005) A New Method For Quantifying The Complexity Of Muscle Attachment Sites. *Anatomical Record (Part B)*, 286B: 21–28.

Appendix 1. Roughness parameters, chord measurements and condylar width by individuals (R = right, L = left)

Skeleton	Side	2 categories	5 categories	Rq_x	Relative length x	Peak number x	Rq_y	Relative length y	Peak number y	Condylar width (mm)	Chord x (mm)	Chord y (mm)
F101	L	1	1	0.809	1.00207	0.075	0.584	1.01249	0.075	44.77	12.76	14.23
F116	R	1	1				1.293	1.03191	0.071	50.68		15.8
F147	L	1	1	0.538	0.99971	0.054	0.428	1.00631	0.066	47.12	15.83	16.21
F172	R	1	1	0.683	1.00677	0.057	0.499	1.02102	0.076	43.62	13.21	14.68
F186	L	1	1	0.91	1.00767	0.065	0.56	1.02071	0.064	45.86	13.4	14.94
F209	R	1	1	0.763	1.01558	0.069	0.336	1.00667	0.064	46.18	13.21	15.7
F252	R	1	1	0.568	1.00549	0.067	0.36	1.00615	0.074	39.96	15.28	13.73
F292	R	1	1				0.639	1.02103	0.068	47.42		13.39
F296	R	1	1	0.761	1.02652	0.073	0.372	1.01363	0.06	48.59	10.31	15.9
F35	L	1	1	0.49	1.00253	0.073						10.53
F43	R	1	1	0.952	1.02045	0.07	0.519	1.00817	0.058	49.11	13.75	16.67
F67	L	1	1	0.379	0.99812	0.084	0.412	1.00213	0.081	46.84	11.49	11.3
F96	R	1	1	0.488	1.01054	0.068	0.576	1.0107	0.063	45.08	15.55	14.78
F233	R	4	21	1.884	1.0219	0.068	0.963	1.01767	0.073	44.96	13.26	14.92
F73	L	4	21	1.346	1.03625	0.063	0.562	1.0128	0.07	47.96	16.7	18.11
F77	R	4	21	0.699	1.01388	0.064	0.598	1.0156	0.052	49.67	12.71	17.92
F90	R	4	21	1.253	1.00456	0.062	0.41	1.00758	0.059	48.08	12.98	15.66
F102	R	4	22	0.814	1.00706	0.071	0.572	1.01468	0.066	42.19	10.19	13.69
F120	R	4	22	1.083	1.02052	0.065	0.386	1.00767	0.065	47.99	13.59	18.77
F13	L	4	22	1.06	1.02801	0.061	0.443	1.01982	0.063	47.5	12.17	14.62
F146	R	4	22	0.903	1.03309	0.08	0.515	1.01083	0.072	44.91	11.07	12.84
F164	R	4	22	0.745	1.01934	0.061	0.653	1.01997	0.063	52.81	15.68	17.49
F175	R	4	22	0.92	1.01706	0.059	0.309	1.00526	0.061	48.11	13.34	16.93
F204	L	4	22	1.194	1.0338	0.065	0.741	1.02065	0.063	44.84	14.02	15.51
F219	L	4	22	0.826	1.01833	0.065	0.35	1.00622	0.067	46.97	6.57	10.04
F260	L	4	22	1.108	1.02788	0.07					13.69	
F28	L	4	22	1.16	1.0211	0.07	0.854	1.02611	0.071	54.24	16.24	19.42
F303	L	4	22	0.555	1.01357	0.07	0.513	1.0177	0.064	51.51	15.11	18.02
F34	L	4	22				0.664	1.02366	0.069	50.62		18.31
F40	R	4	22	0.922	1.02447	0.067	0.868	1.02254	0.069	48.42	13.69	18.12
F60	L	4	22	0.533	1.00351	0.076	0.395	1.01084	0.071	43.65	12.11	12.52
F68	R	4	22	0.706	1.01223	0.063	0.969	1.02807	0.06	46.83	14.09	11.4
F98	R	4	22	0.845	1.01845	0.066	0.653	1.01539	0.064	41.16	13.9	14.32
F86	L	4	23	1.061	1.00938	0.076	0.474	1.01523	0.058	52.16	13.83	17.09

F40, F73, F77, F120, F146, F164, F204 and F233 were all classified as bone formers (Henderson, 2008).